Research Article

Pulmonary Circulation

Protective role of FKBP51 in calcium entry-induced endothelial barrier disruption

Caleb L. Hamilton[1,2], Pierre I. Kadeba[1,2], Audrey A. Vasauskas[3], Viktoriya Solodushko[1], Anna K. McClinton[2,4], Mikhail Alexeyev[2,5], Jonathan G. Scammell[6] and Donna L. Cioffi[1,2]

[1]Department of Biochemistry and Molecular Biology, University of South Alabama, Mobile, AL, USA; [2]Center for Lung Biology, University of South Alabama, Mobile, AL, USA; [3]Department of Anatomical Sciences and Molecular Medicine, Alabama College of Osteopathic Medicine, Dothan, AL, USA; [4]Department of Pharmacology, University of South Alabama, Mobile, AL, USA; [5]Department of Physiology and Cell Biology, University of South Alabama, Mobile, AL, USA; [6]Department of Comparative Medicine, University of South Alabama, Mobile, AL, USA

Abstract

Pulmonary artery endothelial cells (PAECs) express a cation current, I_{SOC} (store-operated calcium entry current), which when activated permits calcium entry leading to inter-endothelial cell gap formation. The large molecular weight immunophilin FKBP51 inhibits I_{SOC} but not other calcium entry pathways in PAECs. However, it is unknown whether FKBP51-mediated inhibition of I_{SOC} is sufficient to protect the endothelial barrier from calcium entry-induced disruption. The major objective of this study was to determine whether FKBP51-mediated inhibition of I_{SOC} leads to decreased calcium entry-induced inter-endothelial gap formation and thus preservation of the endothelial barrier. Here, we measured the effects of thapsigargin-induced I_{SOC} on the endothelial barrier in control and FKBP51 overexpressing PAECs. FKBP51 overexpression decreased actin stress fiber and inter-endothelial cell gap formation in addition to attenuating the decrease in resistance observed with control cells using electric cell-substrate impedance sensing. Finally, the thapsigargin-induced increase in dextran flux was abolished in FKBP51 overexpressing PAECs. We then measured endothelial permeability in perfused lungs of FKBP51 knockout ($FKBP51^{-/-}$) mice and observed increased calcium entry-induced permeability compared to wild-type mice. To begin to dissect the mechanism underlying the FKBP51-mediated inhibition of I_{SOC}, a second goal of this study was to determine the role of the microtubule network. We observed that FKBP51 overexpressing PAECs exhibited increased microtubule polymerization that is critical for inhibition of I_{SOC} by FKBP51. Overall, we have identified FKBP51 as a novel regulator of endothelial barrier integrity, and these findings are significant as they reveal a protective mechanism for endothelium against calcium entry-induced disruption.

Keywords

FKBP51, I_{SOC}, calcium, endothelial barrier, cytoskeleton

Date received: 25 July 2017; accepted: 30 November 2017

Pulmonary Circulation 2018; 8(1) 1–15

DOI: 10.1177/2045893217749987

Endothelial cells line the inside of blood vessels forming a semi-permeable barrier that is critical for blood and tissue homeostasis. Disruption of the endothelial barrier due to formation of inter-endothelial cell gap formation leads to increased permeability.[1] In pulmonary endothelial cells, calcium entry through a store-operated calcium (SOC) channel, ISOC, leads to inter-endothelial cell gap formation and endothelial barrier disruption.[2–4] I_{SOC} is a small, inwardly rectifying current that can be activated by the Ca^{2+}-ATPase blocker thapsigargin.[2–7] While ISOC conducts both calcium and sodium ions, it exhibits anomalous mole fraction

Corresponding author:
Donna L. Cioffi, MSB 2316, Department of Biochemistry and Molecular Biology, 5851 USA Drive N., University of South Alabama, Mobile, AL 36688, USA.
Email: dlcioffi@southalabama.edu

behavior reflecting moderate selectivity for calcium.[2] Indeed, it is calcium permeation which is important for inter-endothelial cell gap formation, as incubation of cells in the absence of extracellular calcium but in the presence of sodium does not lead to thapsigargin-induced gap formation.[8] As such, it would be expected that inhibition of calcium entry through ISOC will preserve the endothelial barrier. However, it has not yet been determined whether inhibition of I_{SOC} is endothelial barrier protective and this was one focus of the current study.

In order to study I_{SOC} inhibition, it is important to first identify interacting proteins that play a role in ISOC channel function. The ISOC channel is tethered to the cytoskeleton and its activation depends upon an intact spectrin–protein 4.1–TRPC4 interaction.[4,6] TRPC4 is a member of the transient receptor potential canonical (TRPC) protein subfamily of the transient receptor potential (TRP) protein superfamily[9] and is likely a pore-forming subunit of the ISOC channel. TRPC4 interacts with TRPC1 as well as with orai1 which influences channel activity and calcium selectivity.[3] More recently, we demonstrated that the large molecular weight immunophilins FKBP51 and FKBP52 are also part of the ISOC channel heterocomplex.[10]

FKBP51 and FKBP52 are members of the FK506-binding protein immunophilin family that are best known for their roles in steroid receptor signaling, where they have opposing effects on receptor function.[11,12] Whereas FKBP52 potentiates steroid receptor activation, FKBP51 inhibits activation. We have shown similar opposing roles of FKBP52 and FKBP51 in calcium signaling.[10] More specifically, FKBP52 promotes thapsigargin-induced calcium entry in rat pulmonary artery endothelial cells (PAECs) whereas FKBP51 inhibits calcium entry through ISOC. As I_{SOC} activation leads to the formation of inter-endothelial cell gaps, the FKBP51-mediated inhibition of I_{SOC} may be of pharmacological value. However, it is unknown whether alteration of FKBP51 levels in PAECs directly affects inter-endothelial cell gap formation and barrier integrity. Addressing this question was the major focus of the current study. To study the relationship between FKBP51 and endothelial barrier function, we generated a PAEC cell line that stably overexpresses FKBP51. Overexpression of FKBP51 led to inhibition of thapsigargin-induced I_{SOC} and preservation of the endothelial barrier as assessed by decreased actin stress fiber formation and decreased inter-endothelial cell gap size and quantity. Additionally, resistance changes measured via electric cell-substrate impedance sensing (ECIS®) were negligible and there was no increase in dextran flux in FKBP51 overexpressing cells following thapsigargin treatment. In situ, Evans Blue dye-conjugated albumin tissue permeation was greater in lungs from FKBP51 knockout ($FKBP51^{-/-}$) mice following calcium entry compared to wild-type (WT) mice. Overall, these data suggest that the physiological role of FKBP51 is to limit calcium entry-induced endothelial barrier disruption.

Mechanisms underlying the effects of FKBP51 on thapsigargin-induced I_{SOC} in PAECs are not yet understood. As FKBP51 has been implicated in regulating microtubule polymerization,[13,14] and ISOC channel function is sensitive to changes in microtubule polymerization,[3] we investigated the role of the microtubule network in the FKBP51-mediated inhibition of I_{SOC}. FKBP51 overexpressing PAECs exhibited a more extensive microtubule network compared to control cells. Cells were then treated with nocodazole at different concentrations to achieve a range of partial to almost complete microtubule depolymerization. At low nocodazole concentrations, which affected only limited microtubule depolymerization, FKBP51 was unable to inhibit I_{SOC}. Thus, FKBP51 regulates microtubule polymerization that is critical for the inhibition of I_{SOC}. Collectively, our observations reveal that FKBP51 is a regulator of endothelial barrier integrity, and by inhibiting I_{SOC} it serves to protect endothelial cells from actin rearrangement and endothelial barrier disruption.

Methods

Reagents

All reagents were obtained from Sigma-Aldrich (St. Louis, MO, USA) unless otherwise noted. Cell culture medium was obtained from Thermo Fisher Scientific (Waltham, MA, USA) or Santa Cruz Biotechnology (Santa Cruz, CA, USA) and penicillin/streptomycin was obtained from Thermo Fisher Scientific. EquaFETAL® bovine serum (EBS) and fetal bovine serum (FBS) were purchased from Atlas Biologicals, Inc. (Fort Collins, CO, USA) and Thermo Fisher Scientific, respectively. Hank's Balanced Salt Solution (HBSS) was purchased from Thermo Fisher Scientific. Monoclonal antibodies to FKBP51 and expression plasmids for human FKBP51 have been described previously.[15,16] β-actin antibody was purchased from Santa Cruz Biotechnology. Doxycycline was purchased from Clontech Laboratories, Inc. (Mountain View, CA, USA).

Cell culture

PAECs were isolated from Sprague-Dawley rats and characterized as described.[17] Cells are grown in high glucose DMEM supplemented with 10% FBS or EBS, penicillin G (50 U/mL), and streptomycin (0.05 mg/mL). Animal work was approved by the University of South Alabama Institutional Animal Care and Use Committee and was performed in compliance with the National Institutes of Health *Guide for the Care and Use of Laboratory Animals*.

FKBP51 overexpressing cells were generated by lentiviral transduction. Production of lentiviral supernatants and infection of target cells was performed as described previously.[18] Briefly, lentivirus containing supernatants were produced by $CaPO_4$-mediated transfection of HEK293FT cell lines using established protocols.[19,20] Gag, Pol, and Env

functions for lentiviral constructs were provided in *trans* by cotransfection of the vector plasmid with two helper plasmids, psPAX2 and pMD2.G (both gifts from Didier Trono [École Polytechnique Fédérale de Lausanne; Addgene (Cambridge, MA, USA)] plasmid #12260 and #12259, respectively). Transduction of PAECs with the lentivirus encoding human FKBP51 (lv3899) was performed in 35-mm dishes at 50% confluence by incubating them overnight with corresponding supernatant in the presence of 10 μg/mL polybrene. The next day, supernatant was removed and cells were allowed to recover for 24 h in fresh DMEM after which they were selected with puromycin (1 μg/mL) for three days.

Quantitative polymerase chain reaction (qPCR)

Messenger RNA was prepared from PAECs using the RNeasy mini kit (Qiagen, Valencia, CA, USA) and reverse transcribed to complementary DNA (cDNA) using an iScript cDNA preparation kit (Bio-Rad Laboratories, Hercules, CA, USA). qPCR was performed by SYBR Green incorporation using a CFX Connect (Bio-Rad) thermocycler with the following primers:

rHPRT1qPCRf 5'-GACCTCTCGAAGTGTTGGATAC-3'
rHPRT1qPCRr 5'-TCAAATCCCTGAAGTGCTCAT-3'
hFKBP51qPCR-1f 5'-GCTGAGCAGGGAGAGGATAT TA-3'
hFKBP51qPCR-1r 5'-TCTCCAATCATCGGCGTTTC-3'

Western blotting

Cells were lysed by scraping and sonification for 10 s (Branson Digital Sonifier model S-450D; Branson, Danbury, CT, USA) at 12% output in RIPA buffer (Boston Bioproducts; Ashland, MA, USA) with 1% protease inhibitor cocktail followed by centrifugation at 12,000× *g* for 20 min. Whole cell lysates were electrophoresed on 4–12% bis-Tris gels (Thermo Fisher Scientific). Proteins were transferred to nitrocellulose membranes at 100 V. Membranes were blocked with milk (5% non-fat dry milk/0.2% BSA in PBS supplemented with 0.1% Tween-20) for 1 h and then rocked with primary antibodies overnight at 4°C and with secondary antibodies for 1 h at room temperature. Supersignal West Pico or West Femto chemiluminescent substrates (Thermo Fisher Scientific) were applied to membranes to allow for protein visualization.

Cytochemistry

Cells were seeded on coverslips and grown to 80–100% confluence in 35-mm dishes. Cells were either fixed immediately or were pretreated with thapsigargin (1 μM) for 5 min before fixation. For actin stress fiber analysis, the cells were fixed with 4% paraformaldehyde for 15 min at room temperature, washed with 100 mM glycine in PBS, then permeabilized with 0.1% Triton X-100 in PBS for 1–2 min. For microtubule analysis, monolayers were fixed and permeabilized with 90% ice-cold methanol in PBS for 3 min at −20°C. Following fixation/permeabilization, cells were incubated in blocking buffer (10% normal goat serum, 10% normal donkey serum, 1.5% glycine, 1% bovine serum albumin in HBSS) for 1 h at room temperature. To visualize filamentous actin, cells were incubated with AlexaFluor 568 phalloidin (Molecular Probes; Eugene, OR, USA) either diluted 1:100 in PBS for 15 min at room temperature or diluted 1:150 in milk (5% non-fat dry milk in PBS supplemented with 0.1% Tween-20) overnight at 4°C. Cells were incubated with Hoechst 33342 nuclear counterstain (500 μM; Thermo Fisher Scientific) under agitation for 20 min at room temperature. To visualize tubulin and EB-1, cells were incubated with primary antibodies diluted in milk (5% non-fat dry milk in PBS supplemented with 0.1% Tween-20) overnight at 4°C. Cells were treated sequentially with secondary antibodies, with a wash in between, for 1 h at room temperature. Dilutions used for primary antibodies were 1:200 for α-tubulin and 1:150 for EB-1. Secondary antibodies were used at 1:500 dilution and include goat anti-mouse IgG fluorescein-conjugated (Thermo Fisher Scientific; Pittsburg, PA, USA) and AlexaFluor 488 donkey anti-goat IgG (H&L) (Life Technologies, Grand Island, NY, USA). Cells were incubated with Hoechst 33342 nuclear counterstain (10 μg/mL; Thermo Fisher Scientific) under agitation for 20 min at room temperature. Cells were incubated with CellMask™ Orange cell membrane stain (5 μg/mL; Life Technologies) under agitation for 40 min at room temperature. Fluorescent images were obtained using a Nikon A1 confocal laser scanning microscope (NIH S10RR027535) fitted with a 60X water immersion objective or a Zeiss Observer.D1 widefield microscope (Carl Zeiss®, Germany) fitted with 40X oil immersion objective.

Global Ca^{2+} measurements and patch-clamp electrophysiology

Cells were seeded onto glass coverslips and grown to confluence in 35-mm dishes. Changes in cytosolic calcium concentration were determined using Fura 2-acetoxymethyl ester (Fura 2/AM; Thermo Fisher Scientific).[4–6,21] Patch-clamp electrophysiology recordings were performed in whole-cell configuration on electrically isolated cells as described.[4] Isolation of single cells was achieved via treatment of cell monolayers with a non-enzymatic cell dissociation solution in PBS (catalog no. C5789). Transmembrane current was measured with an Axopatch 200B Amplifier (Molecular Devices; Sunnyvale, CA, USA). PClamp10 software was used to record the current evoked by step depolarization in 20 mV increments from −100 to +80 mV. Currents were measured as the mean value of the current amplitude during the last 20 ms of each step. The standard pipette solution contained (in mmol/L) 130 N-methyl-D-glucamine, 10 Hepes, 2 Mg^{2+}-ATP, 1 N-phenylanthranilic acid,

0.1 5-nitro-2-(3-phenylpropylamino)benzoic acid, 2 EGTA, 1 $Ca(OH)_2$ (pH 7.2, adjusted with methane sulfonic acid). The bath (external) solution contained (in mmol/L) 120 aspartic acid, 5 $Ca(OH)_2$, 5 $CaCl_2$, 10 Hepes, 0.5 3,4-diaminopyridine (pH 7.4 adjusted with tetraethylammonium hydroxide). All solutions were adjusted to 290–300 mOsm/L with sucrose. The free [Ca^{2+}] was estimated to be 100 nmol/L as previously described.[10] Recording pipettes are made of hemo capillaries (A-M Systems; Sequim, WA, USA) pulled by a micropipette puller (P-97; Sutter Instruments; Novato, CA, USA) and heat-polished by a microforge (MF-830; Narishige; Tokyo, Japan) to a final resistance of 3–5 megaohms when filled with standard pipette solution. All of the experiments were performed at room temperature (22–25°C). Data are expressed as mean ± SEM for the number of cells (*n*) in which whole-cell patch-clamp recordings were obtained. Average change in overall current was calculated by summing the average change at each testing potential and dividing by 10 (the number of testing potentials used).

Actin stress-fiber quantification

Cells were seeded onto triplicate 24-well plates and grown to confluence. Each cell type was seeded into ten wells of the respective 24-well plate. The corner wells were treated with cell-free endothelial cell media. The WT and constitutive FKBP51 overexpressing PAEC monolayers were treated with either 1 μM thapsigargin in DMSO or the equivalent volume of DMSO without thapsigargin in media for 20 min. The monolayers were paraformaldehyde-fixed, permeabilized, and subjected to cytochemistry using AlexaFluor 568 phalloidin as described above. Nuclear counterstain was also applied as an internal control for cell count. The cell-free corner wells were also treated with the above conditions. Fluorescence at 620-nm and 460-nm wavelengths was recorded in each well simultaneously with a Synergy 2 fluorescence plate reader (BioTek; Winooski, VT) using with Gen5 (BioTek) software. The mean fluorescence from the cell free corner treatments was subtracted from the average fluorescence of treatment at each wavelength measured.

EB-1 microtubule plus-end quantification

Cells were seeded onto glass coverslips in 35-mm dishes, grown to confluence and treated with either 1 μM thapsigargin in DMSO or the equivalent volume of DMSO without thapsigargin in media for 20 min. The monolayers were methanol-fixed, permeabilized, and subjected to immunocytochemistry for EB-1 as described above. In addition to the Hoechst nuclear counterstain, the monolayers were also treated with CellMask™ Orange cell membrane stain. Cell monolayers were imaged via a Nikon A1 confocal microscope. Images were analyzed with Image J software. Green fluorescent events above a constant threshold for all treatments were obtained. The relative distance of each detected event between the nuclear membrane (parameters determined by the nuclear counterstain) and the cell membrane (parameters determined by the cell membrane stain) of each image was calculated.

Gap formation studies and electric cell-substrate impedance sensing (ECIS®)

Constitutive FKBP51 overexpressing PAECs and WT PAECs were seeded onto 35-mm coverslips and grown to confluence. Cells were imaged (40X oil immersion) at 5-s intervals for 60 min using a Zeiss Observer.D1 widefield microscope and AxioVision Rel 4.8 Software. Thapsigargin (1 μM) was added 5 min after the beginning of experiments. Gap size was measured by outlining gap areas and using the pixel-to-micron conversion feature of the AxioVision Rel 4.8 Software.

ECIS® experiments were performed as previously described.[22] Baseline resistance measurements were obtained for at least 30 min. Thapsigargin (1 μM) was then added to each well to initiate calcium entry. Change in resistance was measured until a new baseline was obtained.

Transwell dextran-flux assays

Endothelial cells were cultured in growth medium on a porous polycarbonate membrane (Corning Incorporated; Corning, NY, USA; Costar Transwell #3413) to confluency. Experiments were initiated by adding 330 μg/mL of 40,000 Da FITC-Dextran or 330 μg/mL FITC-Dextran/1 μM thapsigargin mix to the upper chamber, and the increase in intensity of FITC-Dextran was measured in the lower chamber over time using the Synergy 2 (BioTek) multi-mode microplate reader.

In situ endothelial permeability measurement

$FKBP51^{-/-}$ mice were purchased from The Jackson Laboratory (Bar Harbor, ME, USA). For these mice, a *lacZ* targeting vector replaces the first coding exon of the *Fkbp5* gene. WT mice used in these experiments were littermates of the $FKBP51^{-/-}$ mice.

Male and female mice aged 10–12-weeks (20–25 g) were used in this study. To perform the in-chest lung perfusion protocol,[23] anesthetized mice were weighed and tracheostomized. Lungs were exposed by removal of the anterior chest wall and cannulas inserted in the pulmonary artery and left ventricle. Lungs were then perfused *in situ* under constant flow (2 mL/min) without recirculation with 4% bovine serum albumin (BSA) in HBSS buffer containing 2 mM Ca^{2+} at 37°C for 15 min after which they were challenged with 30 nM thapsigargin for 15 min. Finally, 2.5 mL (0.1 g dye/5% BSA) albumin-bound Evans Blue were added to 45 mL perfusate for an additional 15 min. Lungs were then excised, blotted dry, weighed, and homogenized in PBS ($1\,mL \cdot 100\,\mu g^{-1}$ tissue) and incubated with two volumes

of formamide (18 h, 60°C) followed by centrifugation at 12,000 × *g* for 20 min. Optical density of the supernatant was determined by spectrophotometry at 620 nm.

Statistical analysis

Statistical analysis was performed using GraphPad version 5.0 software (San Diego, CA, USA). Data are presented as mean ± SEM. Comparisons between multiple groups were performed using a two-way ANOVA and the Bonferroni post hoc test. Student's *t*-tests were used elsewhere. Values were considered significantly different when $P < 0.05$. Sample size for *in vitro* experiments is the number of independent experiments using independently passaged cell cultures. For *in situ* experiments, we used the minimum number of animals required to achieve statistical significance.

Results

Characterization of I_{SOC} and actin stress fiber formation in PAECs

Thapsigargin, a plant alkaloid, causes emptying of the endoplasmic reticulum calcium store by blocking the SERCA Ca^{2+}/ATPase pump.[24] In PAECs, thapsigargin treatment leads to global calcium entry that is sensitive to 2-aminoethoxydiphenyl borate (2-APB) and YM-58483.[25] While both 2-APB and YM-58483 are SOC entry inhibitors, 2-APB is considered to be relatively non-specific,[26] whereas YM-58483 is a potent inhibitor of the I_{CRAC} (calcium release activated calcium current).[27] We were particularly interested in 2-APB because it blocks calcium entry through some TRPC channels,[28–30] and the endothelial ISOC channel is composed of at least TRPC1 and TRPC4 subunits.[5,31] Xu et al.[25] showed that treatment of PAECs with 2-APB resulted in a ~50% decrease in thapsigargin-induced global calcium entry. Similarly, YM-58483 decreased global calcium entry by ~50%, overall suggesting that thapsigargin activates multiple calcium entry pathways in PAECs. Indeed, one of these pathways is I_{SOC};[2,3,5–7] however, it is unknown whether I_{SOC} is sensitive to 2-APB or YM-58483. We thus performed patch-clamp electrophysiology to measure I_{SOC} in the presence of 2-APB or YM-58483. Thapsigargin treatment activated I_{SOC}, a small current of -22.8 ± 2.5 pA at –40 mV that has a reversal potential of ~ + 32 mV (Fig. 1a), and lanthanum reduced the current to noise level, consistent with that previously reported.[4] 2-APB reduced I_{SOC} by ~46% (average

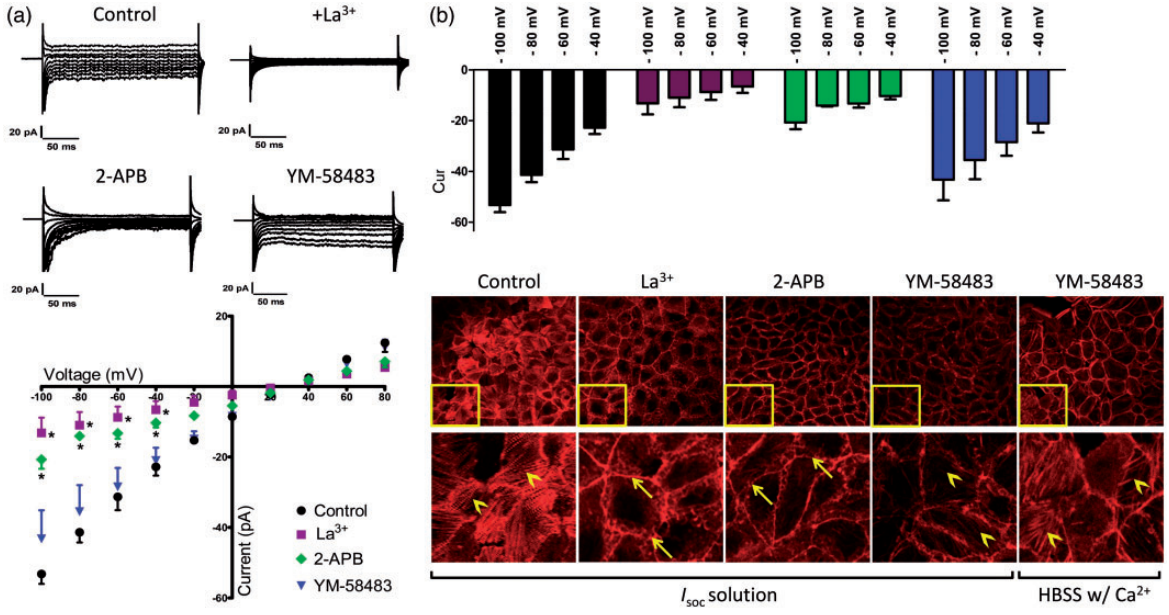

Fig. 1. I_{SOC} inhibition is associated with decreased actin stress fiber formation. (a) (Top) Current tracings of I_{SOC} activated by thapsigargin (1 μM) at testing potentials -100 mV to +80 mV. (Bottom) Corresponding *I*/V curves. In control PAECs or PAECs treated with the I_{CRAC} blocker YM-58483 (10 μM[25]), thapsigargin activates a normal I_{SOC}. In PAECs treated with La^{3+} (50 μM[5]) or the store-operated channel blocker 2-APB (75 μM[25]), I_{SOC} was significantly decreased. *$P < 0.05$ for 2-APB vs. control and La^{3+} vs. control; n = 3. (b) Cytochemistry staining for actin stress fibers reveals stress fiber formation in PAECs only when I_{SOC} is activated. (Top) Maximum I_{SOC} currents are shown at each testing potential under different conditions. (Bottom: top panel) Whole field view of PAECs treated with thapsigargin and stained for actin stress fibers. Cells were bathed in the same solution (I_{SOC} solution) used in patch-clamp electrophysiology so that upon thapsigargin application cation current was reflective of calcium entry. PAECs were also treated with YM-58483 when in non-selective solution, HBSS + Ca^{2+} (1.3 mM). (Bottom: bottom panel) Expanded view of inset from top panel. Thapsigargin-induced I_{SOC} resulted in actin stress fiber formation (arrowheads) in control PAECs and in PAECs treated with I_{CRAC} blocker YM-58483. However, stress fiber formation was prevented and cortical actin maintained (arrows) when cells were treated with La^{3+} or 2-APB, which block I_{SOC}. Images were acquired at 40X magnification. Images shown are representative of n = 3.

differences at all testing potentials) whereas YM-58483 had no appreciable effect. The observation that I_{SOC} is sensitive to 2-APB but not YM-58483 is consistent with TRPCs 1 and 4 contributing to the ISOC channel make-up.

We next wanted to determine whether inhibition of I_{SOC} leads to decreased thapsigargin-induced stress fiber formation. It was previously shown that thapsigargin treatment of PAECs leads to downstream actin stress fiber and inter-endothelial cell gap formation.[8] As thapsigargin activates multiple calcium entry pathways, it was not clear whether the I_{SOC} pathway in particular is important for actin stress fiber formation. To address this question, we performed cytochemistry of thapsigargin-treated PAEC monolayers using Rhodamine-phalloidin to visualize actin filaments. To rule out contributions from other ionic currents, e.g. Cl^-, K^+ and Na^+, the cells were bathed in the same solution (which we refer to as I_{SOC} solution) that is used for patch-clamp electrophysiology. In this way, any stress fiber formation that occurs will be the result of calcium current. Additionally, cells were treated with the I_{SOC} inhibitors, La^{3+} and 2-APB, or with the I_{CRAC} inhibitor YM-58483. In PAECs treated with thapsigargin, I_{SOC} was activated and actin stress fibers formed throughout the monolayer (Fig. 1b). In the presence of La^{3+} or 2-APB, both of which inhibited I_{SOC}, thapsigargin-induced actin stress fiber formation was abolished. In the presence of YM-58483, which did not inhibit I_{SOC}, actin stress fibers still formed, although at decreased levels compared to control PAECs. We also tested YM-58483 when the cells were bathed in HBSS with calcium instead of the I_{SOC} solution. Here in the presence of YM-58483, again we observed actin stress fiber formation. Overall, these observations suggest that calcium entry must occur through specific channels, one in particular being the ISOC channel, for actin stress fibers to form. As I_{SOC} activation leads to actin stress fiber and inter-endothelial cell gap formation,[7] inhibition of I_{SOC} should be protective to the endothelial barrier. Indeed, here we show that inhibition of I_{SOC} correlates with decreased stress fiber formation. A caveat however is that both La^{3+} and 2-APB can block other channels in addition to the ISOC channel. We have identified another I_{SOC} inhibitor, the immunophilin FKBP51,[10] although it has not yet been determined whether inhibition of I_{SOC} by FKBP51 is protective to the endothelial barrier

Increased FKBP51 expression inhibits I_{SOC} in PAECs

We have previously demonstrated that treatment of PAECs with dexamethasone upregulates FKBP51 expression leading to decreased thapsigargin-induced I_{SOC}.[10] In that study we also demonstrated FKBP51-mediated inhibition of I_{SOC} in doxycycline-inducible FKBP51 HEK293 cells. However, to be certain that the dexamethasone effect on I_{SOC} in PAECs was specifically due to FKBP51 upregulation, in the current study we generated via lentiviral construct a PAEC cell line that constitutively overexpresses FKBP51 (cFKBP51). This cell line also gave us a tool to study the effect of FKBP51 on endothelial barrier function. qPCR and western blot analysis confirmed upregulation of FKBP51 (Fig. 2a and b). At the protein level, FKBP51 expression was increased by 3.1 ± 0.5-fold compared to control cells. Using whole cell patch-clamp electrophysiology, I_{SOC} was decreased by ~40% in the FKBP51 overexpressing cells compared to control cells (Fig. 2c).

We then measured global calcium entry following thapsigargin treatment using the ratiometric dye Fura 2/AM. Using a calcium add-back approach, we observed that cFKBP51 PAECs exhibited calcium entry that was not statistically different from control cells (Fig. 2d and e). Whereas increased FKBP51 expression in PAECs does not change the global calcium entry, it does inhibit I_{SOC}. Taking into consideration that measurement of global calcium reflects calcium entry through all thapsigargin-activated calcium channels, these observations suggest that FKBP51 is principally acting on the ISOC channel and not other calcium entry channels.

Increased FKBP51 expression inhibits calcium entry-induced stress fiber formation

As we have shown that FKBP51 is principally inhibiting calcium entry through the ISOC channel in PAECs, we next went on to determine whether inhibition of I_{SOC} by FKBP51 decreases thapsigargin-induced stress fiber formation. Here, WT and cFKBP51 PAECs were grown to confluence, treated with thapsigargin to activate calcium entry, fixed, permeabilized, and stained with AlexaFluor 568 phalloidin to visualize filamentous actin. In control PAECs without thapsigargin treatment, actin was principally localized to the cell periphery as the cortical actin rim (Fig. 3a, top left). Following thapsigargin treatment, actin stress fibers appeared throughout the monolayer (Fig. 3a, bottom left). In cFKBP51 PAECs, there was very little thapsigargin-induced actin stress fiber formation (Fig. 3a, compare top and bottom right). Quantitation of filamentous actin (F-actin) using phalloidin revealed a $21 \pm 7\%$ increase in F-actin in control PAECs following thapsigargin treatment, reflective of stress fiber formation (Fig. 3b). On the other hand, thapsigargin had no effect on F-actin in cFKBP51 cells. Overall, these data indicate that inhibition of I_{SOC} by FKBP51 decreases calcium entry-induced actin stress fiber formation.

Increased FKBP51 expression leads to increased microtubule polymerization in PAECs

We have shown that FKBP51 inhibits I_{SOC} and downstream actin stress fiber formation. In endothelial cells, there is cross-talk between the actin and microtubule networks where microtubule depolymerization precedes actin stress fiber formation[32,33] and microtubule stabilization decreases actin stress fiber formation.[34,35] Further, FKBP51 was

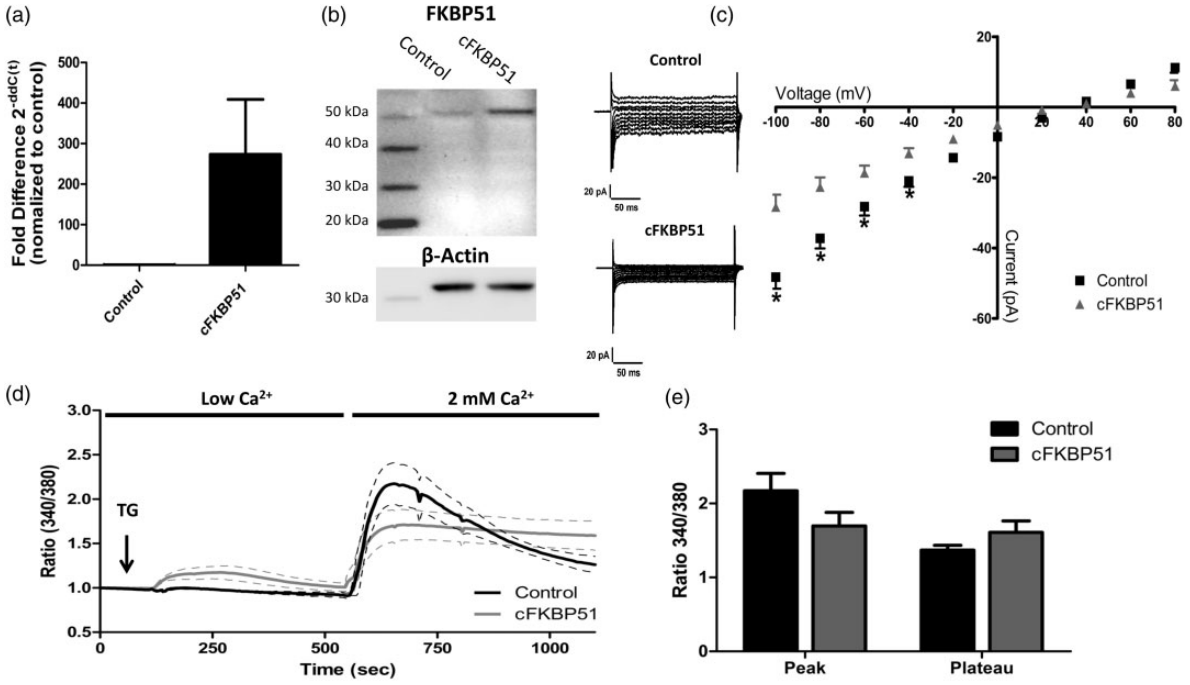

Fig. 2. FKBP51 overexpression inhibits I_{SOC} in PAECs. (a, b) PAECs were engineered to constitutively overexpress human FKBP51 (cFKBP51). qPCR analysis (a) and immunoblotting (b) indicate upregulation of FKBP51. Densitometry of protein bands revealed that relative to actin, FKBP51 expression was increased 3.1 ± 0.5-fold in the cFKBP51 cells compared to control cells. $n = 6$ for qPCR data. Immunoblot shown is representative of $n = 3$. (c) I_{SOC} was measured using patch-clamp electrophysiology. (Left) Current tracings of I_{SOC} activated by thapsigargin (1 μM) at testing potentials −100 mV to +80 mV. (Right) Corresponding *I*/V curves. The current in cFKBP51 cells was decreased ~40% compared to control cells. $^*P < 0.05$; $n = 6$. (d) Global calcium entry was measured using the ratiometric dye Fura 2/AM and the calcium add-back protocol. Addition of thapsigargin (1 μM, TG) in low extracellular calcium reveals release of calcium from the endoplasmic reticulum. Add-back of 2 mM Ca^{2+} reveals calcium entry. Each tracing represents the average of at least four experiments. (e) Bar graph comparing calcium entry between cFKBP51 and control cells both at the peak (maximum) response as well in the plateau region following the peak region. There was no difference in global calcium entry responses between cFKBP51 and control PAECs.

shown to promote microtubule polymerization in a *Xenopus* oocyte system.[14] Thus, we questioned whether microtubules are playing a role in FKBP51's effect on I_{SOC}. We first wanted to determine whether increased FKBP51 expression promotes microtubule polymerization in PAECs. Immunoblotting was performed for total and tyrosinated tubulin in control and cFKBP51 PAECs. Tyrosination is a post-translational modification that occurs on α-tubulin,[36] and detyrosinated microtubules exhibit enhanced stability.[37] While total tubulin levels did not differ between the two cell types, cFKBP51 cells exhibited decreased tyrosinated tubulin ($46 \pm 7\%$), suggesting more detyrosinated tubulin and increased microtubule stability (Fig. 4a).

Immunocytochemistry was then performed to visualize the microtubule cytoskeletal network. In contrast to WT PAECs which showed microtubules extending from the centrosome partially into the cytosol, the cFKBP51 cells exhibited a much more extensive microtubule network throughout the entire cytosol, suggesting increased microtubule polymerization (Fig. 4b). To quantitatively confirm the more extensive microtubule network in cFKBP51 cells, the number of the microtubule plus-ends and their spatial orientation relative to the nucleus and the plasma membrane were measured. Here, microtubule plus-ends were identified using EB-1 antibody, and we observed that microtubules in cFKBP51 cells were more numerous and extended farther away from the nucleus as compared to control PAECs, overall revealing increased microtubule polymerization in the cFKBP51 cells (Fig. 4c and d). Further, following a 20-min thapsigargin treatment, the number and localization of microtubule plus-ends were not different than the respective vehicle treatment in both WT and cFKBP51 PAECs. Overall, we have determined that FKBP51 impacts microtubule dynamics in PAECs by increasing microtubule polymerization.

FKBP51 inhibits I_{SOC} through microtubule polymerization

We next wanted to determine whether microtubule polymerization by FKBP51 leads to inhibition of I_{SOC}. To address this question, we treated WT or cFKBP51 PAECs with nocodazole over a concentration range that effected limited to complete dissolution of the microtubule network. In the absence of nocodazole, cFKBP51 PAECs again exhibited a more extensive microtubule network than WT cells (Fig. 5a). With a 10-μM nocodazole treatment,

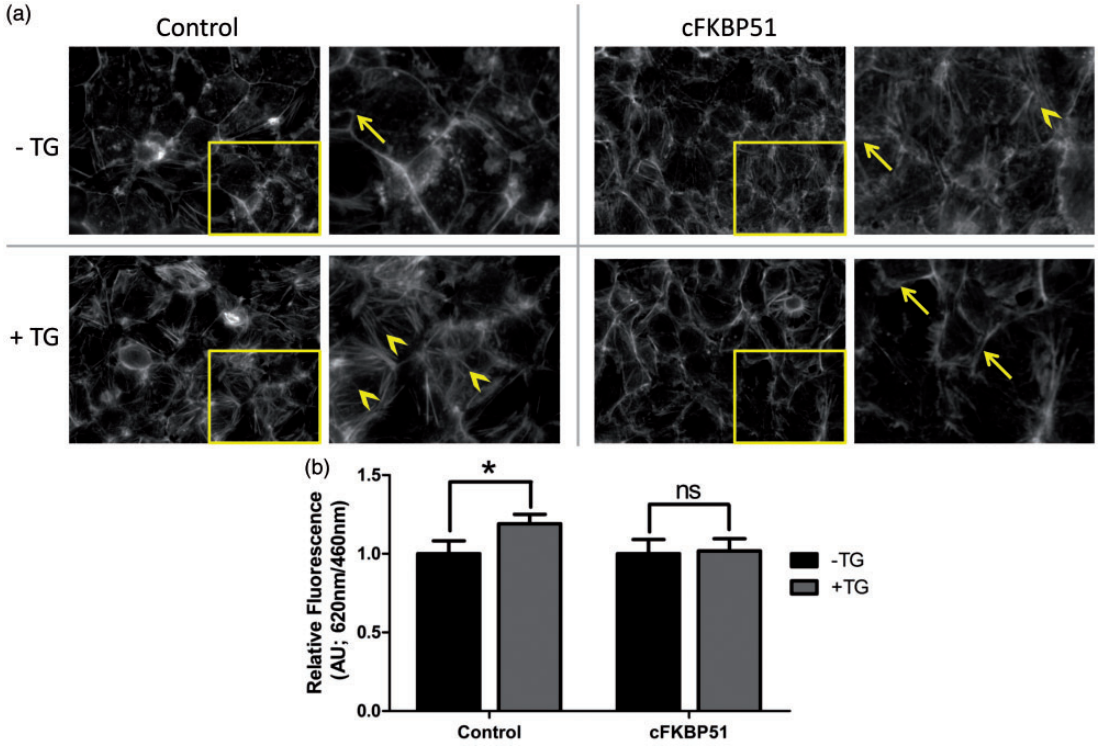

Fig. 3. FKBP51 overexpression inhibits actin stress fiber formation in PAECs. (a) Control and cFKBP51 PAECs were treated with thapsigargin (1 μM, TG) and then stained with AlexaFluor 568 phalloidin to visualize actin filaments. Yellow insets are expanded to the right. In both control and cFKBP51 PAECs not treated with thapsigargin, actin was principally localized to the cortical actin rim (arrows). While thapsigargin treatment resulted in formation of actin stress fibers (arrowheads) in control cells, there was no stress fiber formation in cFKBP51 cells. (b) Quantitation of actin filaments. Upon thapsigargin treatment, actin filaments increased by 21 ± 7% in control PAECs, reflective of stress fiber formation, while there was no increase in cFKBP51 cells. Data were analyzed via Student's *t*-test. $^*P < 0.05$; n = 5.

the microtubule network in WT PAECs was dramatically reduced, and at 100 μM nocodazole, the network was completely disrupted. In cFKBP51 cells, at 10 μM nocodazole, the extended microtubule network was slightly retracted from the cell periphery, but was largely still intact. At 100 μM nocodazole, the microtubule network was mostly condensed to the perinuclear region. We then measured I_{SOC} under these same conditions to determine whether extended microtubules are required for the FKBP51-mediated inhibition of I_{SOC}.

In the WT PAECs, in the absence of nocodazole, a normal I_{SOC} was recorded (Fig. 5b). In the presence of 1 and 10 μM nocodazole, I_{SOC} was decreased in a concentration-dependent manner. At 100 μM nocodazole, with complete dissolution of the microtubule network, the cells could not be patched because a gigaseal could not be attained. When WT PAECs were treated with taxol (10 μM) to stabilize microtubules, I_{SOC} was also decreased. Thus, we observed that I_{SOC} function is dependent on microtubules, which is in agreement with previous observation.[3] If the extended microtubules in cFKBP51 cells are required for inhibition of I_{SOC}, then we would expect that when microtubules are partially depolymerized, inhibition of I_{SOC} will be prevented. Indeed, we observed that when cFKBP51 cells were treated with 1 μM nocodazole, I_{SOC} inhibition was decreased, as evidenced by an increased current, and at 10 μM nocodazole I_{SOC} inhibition was completely prevented (Fig. 5c). To better visualize this, currents recorded at –60 mV holding potential under the conditions of 0 μM nocodazole and 10 μM nocodazole were plotted (Fig. 5d). At 0 μM nocodazole, the current in cFKBP51 PAECs was decreased compared to control cells revealing the FKBP51-mediated inhibition of I_{SOC}. However, at 10 μM nocodazole, FKBP51 was not able to inhibit I_{SOC}, as the current recorded in cFKBP51 cells in 10 μM nocodazole was not significantly different from the current recorded in WT cells with no nocodazole treatment. These data demonstrate that I_{SOC} in PAECs is dependent upon a delicate balance of microtubule polymerization, and that increased microtubule polymerization observed in cFKBP51 PAECs is required for the FKBP51-mediated inhibition of I_{SOC}.

Increased FKBP51 expression reduces calcium entry-induced endothelial permeability

Since we observed that increased FKBP51 expression promotes microtubule polymerization and decreases calcium

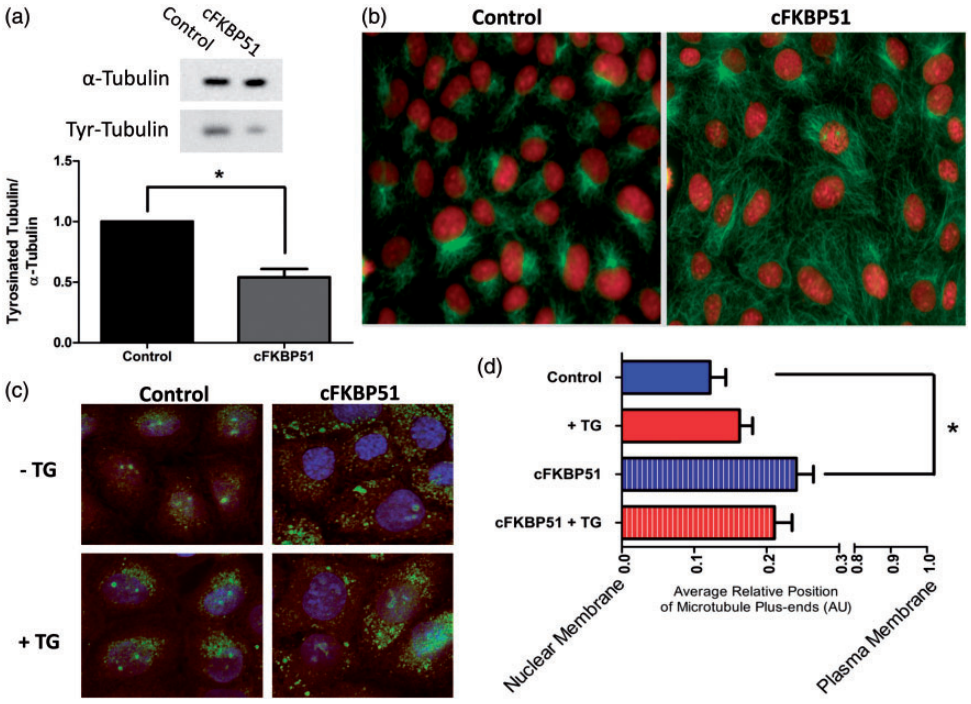

Fig. 4. Increased FKBP51 expression promotes microtubule polymerization in PAECs. (a) (Top) Immunoblots of total tubulin (α-Tubulin) and tyrosinated tubulin (Tyr-Tubulin) in cFKBP51 and control cells. While there was no difference in total tubulin expression between the two cell types, tyrosinated tubulin expression was decreased (46 ± 7%) in the cFKBP51 cells compared to control PAECs. (Bottom) Bar graph showing the tyrosinated to total tubulin densitometry ratios. The trend towards decreased tyrosinated tubulin in cFKBP51 cells is reflective of increased microtubule stability. *$P < 0.05$. Blots are representative of n = 3. (b) Immunocytochemistry showing increased microtubule extensiveness in the cFKBP51 cells compared to control PAECs. In control cells, the microtubule network extended from the perinuclear region and partly into the cytosol, but did not extend out toward the cell periphery. In the cFKBP51 cells, the microtubules were homogeneously distributed throughout the cytosol and extended out towards the cell periphery. Images are representative of n = 3. (c) Cytochemistry of microtubule plus ends. EB-1 (green) identifies microtubule plus ends. Nuclei were stained with Hoechst (blue) and cell membranes were stained with CellMask™ Orange. cFKBP51 cells +/− thapsigargin (TG, 1 μM) exhibited more microtubule plus ends that were distributed throughout the cytosol as compared to control PAECs. Images were acquired at 40X magnification. (d) The positions of the microtubule plus ends were determined relative to the nuclear and plasma membranes. The microtubule plus-ends of the cFKBP51 cells extended closer to the plasma membrane compared to control PAECs. Thapsigargin treatment did not change the plus end positions. *$P < 0.05$; n = 5.

entry-induced actin stress fiber formation, we next questioned whether inter-endothelial cell gap formation is also reduced. Here, confluent monolayers of control and cFKBP51 PAECs were treated with thapsigargin and inter-endothelial cell gap formation was monitored via videomicroscopy over 45 min (Fig. 6a). Time 0 min represents the cells under resting conditions, 5 min before the addition of thapsigargin. Quantitation of inter-endothelial cell gaps revealed that in the basal state, cFKBP51 cells exhibited fewer and smaller gaps compared to control PAECs, suggesting a tighter basal barrier in the cFKBP51 cells (Fig. 6b). Following thapsigargin treatment, there was an increase in inter-endothelial cell gaps in both cell types. However, the cFKBP51 PAECs exhibited fewer and smaller gaps than control cells, revealing a protective effect of FKBP51 on the endothelial barrier. We also performed ECIS® as a measure of endothelial barrier integrity. Following thapsigargin treatment, control PAECs exhibited a decrease in resistance of 17 ± 2% whereas cFKBP51 cells exhibited 7 ± 3% decrease in resistance (Fig. 7a–c), indicating less endothelial barrier disruption as compared to control cells. Finally, we performed dextran flux assays using 40 kD dextran to measure macromolecular permeability across the endothelial barrier. Treatment with thapsigargin resulted in increased permeability in control PAECs whereas there was no permeability increase in cFKBP51 cells (Fig. 7d). Overall, these data reveal that FKBP51 protects the endothelial barrier from calcium entry-induced disruption.

Knockout of FKBP51 exacerbates calcium entry-induced endothelial permeability in situ

As we have shown that overexpression of FKBP51 reduces calcium entry-induced endothelial barrier disruption, we wanted to determine whether knockout of FKBP51 leads to increased endothelial barrier disruption. For this we used FKBP51$^{-/-}$ mice and measured lung endothelial

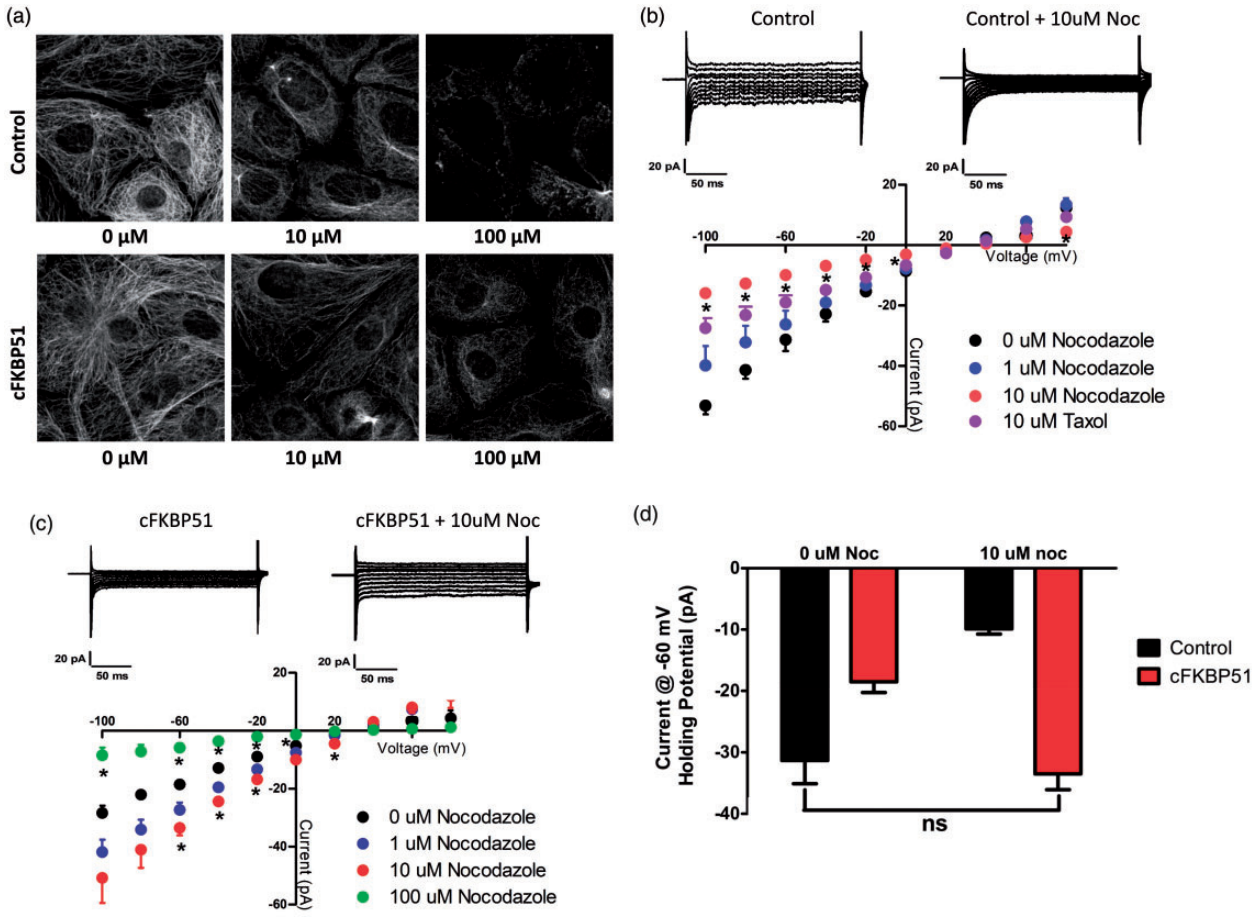

Fig. 5. FKBP51 inhibits I_{SOC} through microtubule polymerization. (a) Control and cFKBP51 PAECs were treated with nocodazole at 10 μM and 100 μM. Control PAECs treated with 10 μM nocodazole exhibited a partially collapsed microtubule network whereas treatment with 100 μM nocodazole completely disrupted the microtubule system. In the cFKBP51 cells treated with 10 μM nocodazole, the microtubule system showed a limited retraction from the cell periphery which was enhanced at 100 μM nocodazole. Visually, the microtubule network of cFKBP51 cells treated with 10 μM nocodazole looked similar to untreated control cells. Images were acquired at 40X magnification. Images are representative of n = 4. (b) (Top) Current tracings of I_{SOC} activated by thapsigargin (1 μM) at testing potentials −100 mV to +80 mV for control PAECs in the presence or absence of 10 μM nocodazole. (Bottom) *I*/V curves of I_{SOC} in control PAECs treated with 0, 1, and 10 μM nocodazole, or 10 μM taxol. I_{SOC} in control PAECs treated with nocodazole at 1 and 10 μM was decreased in a concentration-dependent manner. Cells treated with 100 μM nocodazole were unable to be patched. I_{SOC} was also decreased in taxol (10 μM) treated cells. (c) (Top) Current tracings of I_{SOC} activated by thapsigargin (1 μM) at testing potentials −100 mV to +80 mV for cFKBP51 PAECs in the presence or absence of 10 μM nocodazole. (Bottom) *I*/V curves of I_{SOC} in cFKBP51 PAECs treated with 0, 1, 10, and 100 μM nocodazole. Whereas I_{SOC} in control PAECs was decreased at 1 and 10 μM nocodazole, I_{SOC} in cFKBP51 cells was increased at these concentrations. At 10 μM nocodazole I_{SOC} was restored to that of untreated control cells. At 100 μM nocodazole, I_{SOC} was decreased. $^*P < 0.05$ when compared to current at 0 μM nocodazole; n = 3. (d) The currents recorded at −60 mV holding potential under the conditions of 0 μM nocodazole and 10 μM nocodazole were plotted. At 0 μM nocodazole, the current in cFKBP51 PAECs was inhibited compared to control cells revealing the FKBP51-mediated inhibition of I_{SOC}. However, at 10 μM nocodazole, the FKBP51-mediated inhibition of I_{SOC} was completely abolished in the cFKBP51 PAECs.

permeability *in situ*. Here, we performed an in-chest lung perfusion protocol[23] in WT and FKBP51$^{-/-}$ mice. Thapsigargin was perfused to activate calcium entry and was followed by perfusion of Evans Blue dye-conjugated albumin. Tissue permeation of Evans Blue dye-conjugated albumin was measured as an indicator of endothelial permeability. Lungs from FKBP51$^{-/-}$ mice exhibited ~3 times greater permeability following thapsigargin treatment compared to WT mice (Fig. 8), suggesting that the physiological role of the FKBP51-mediated inhibition of I_{SOC} is to limit calcium entry-induced endothelial barrier disruption.

Discussion

Activation of I_{SOC} in pulmonary endothelium leads to the formation of inter-endothelial cell gaps and endothelial barrier disruption.[7] One paradigm holds that calcium entry causes actin stress fiber formation which then leads to inter-endothelial cell gap formation. Indeed, Moore et al.[8] demonstrated that thapsigargin-induced calcium entry is upstream of actin stress fiber formation and inter-endothelial cell gap formation in PAECs. Similarly, Murphy et al.[38] showed that thrombin-mediated actin

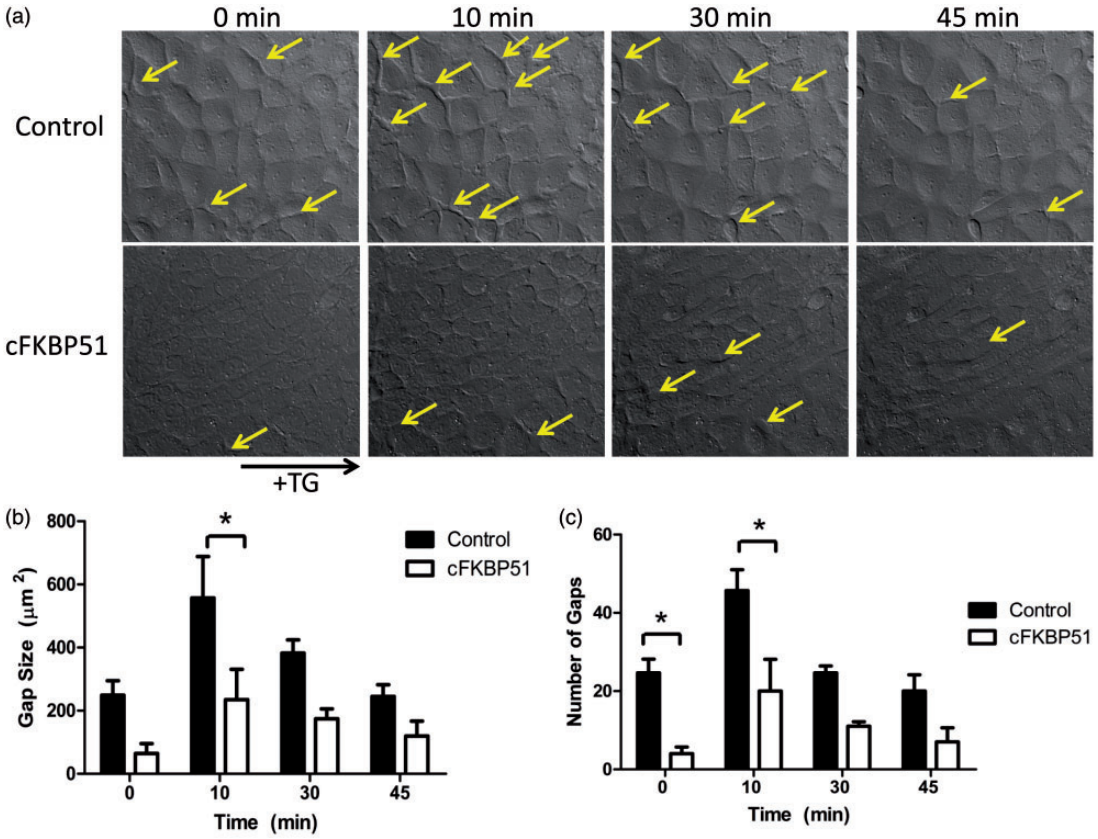

Fig. 6. FKBP51 overexpression inhibits inter-endothelial cell gap formation in PAECs. (a) Control and cFKBP51 PAECs were treated with thapsigargin (1 μM) and inter-endothelial cell gap formation monitored via videomicroscopy. Time 0 min represents the cells under resting conditions, 5 min before the addition of thapsigargin. Arrows indicate areas of inter-endothelial cell gaps. Images were acquired at 40X magnification. (b) Quantitation of size and number of inter-endothelial cell gaps. Under resting conditions, control cells exhibited more gaps than cFKBP51 cells, perhaps suggesting a tighter basal barrier. After thapsigargin treatment, control cells exhibited more and larger gaps than cFKBP51 cells. $^{*}P < 0.05$; $n = 3$.

stress fiber and inter-endothelial cell gap formation are calcium-dependent. An interesting observation in this study was that despite causing large increases in cytosolic calcium, ionomycin did not induce actin stress fiber formation, overall suggesting that calcium must enter through specific channels to initiate actin stress fiber formation. However, several studies have called into question whether actin stress fiber formation is required for calcium-mediated endothelial barrier disruption. In the ionomycin experiment in Murphy et al.'s study,[38] the endothelial barrier was disrupted in the absence of stress fiber formation. In another study using human umbilical vein endothelial cells, Sandoval et al.[39] observed thapsigargin-induced calcium entry and barrier disruption without the formation of actin stress fibers, while thrombin-induced calcium entry did result in the formation of actin stress fibers. More recently, Stolwijk et al.[40] treated human dermal microvascular endothelial cells with thrombin, histamine, and sphingosine-1-phosphate (S1P), all of which activate Gq-linked G protein coupled receptors (GPCRs).[41-43] Actin stress fibers were observed within 2–5 min following thrombin treatment, when the endothelial barrier was disrupted, but the stress fibers became more prominent after 10 min, which coincided with the endothelial barrier recovery phase. In histamine-treated cells, actin stress fibers were not observed until 20 min post treatment, which was after barrier disruption occurred. On the other hand, calcium entry following S1P treatment did not lead to actin stress fiber formation or barrier disruption. Collectively, these studies support the idea that not all increases in cytosolic calcium lead to actin stress fiber formation and further, that endothelial barrier disruption can occur independently of actin stress fiber formation. In the current study, we demonstrate that I_{SOC} activation is a critical determinant of actin stress fiber formation. Indeed, FKBP51 inhibits I_{SOC} but not other calcium entry pathways in PAECs, and FKBP51 prevents thapsigargin-induced actin stress fiber formation. These data implicate I_{SOC} as the calcium entry pathway important for actin stress fiber formation in pulmonary endothelial cells. Further, when I_{SOC} and actin stress fiber formation were inhibited, the endothelial barrier was protected from disruption. Overall, our data indicate that, at least in pulmonary endothelial

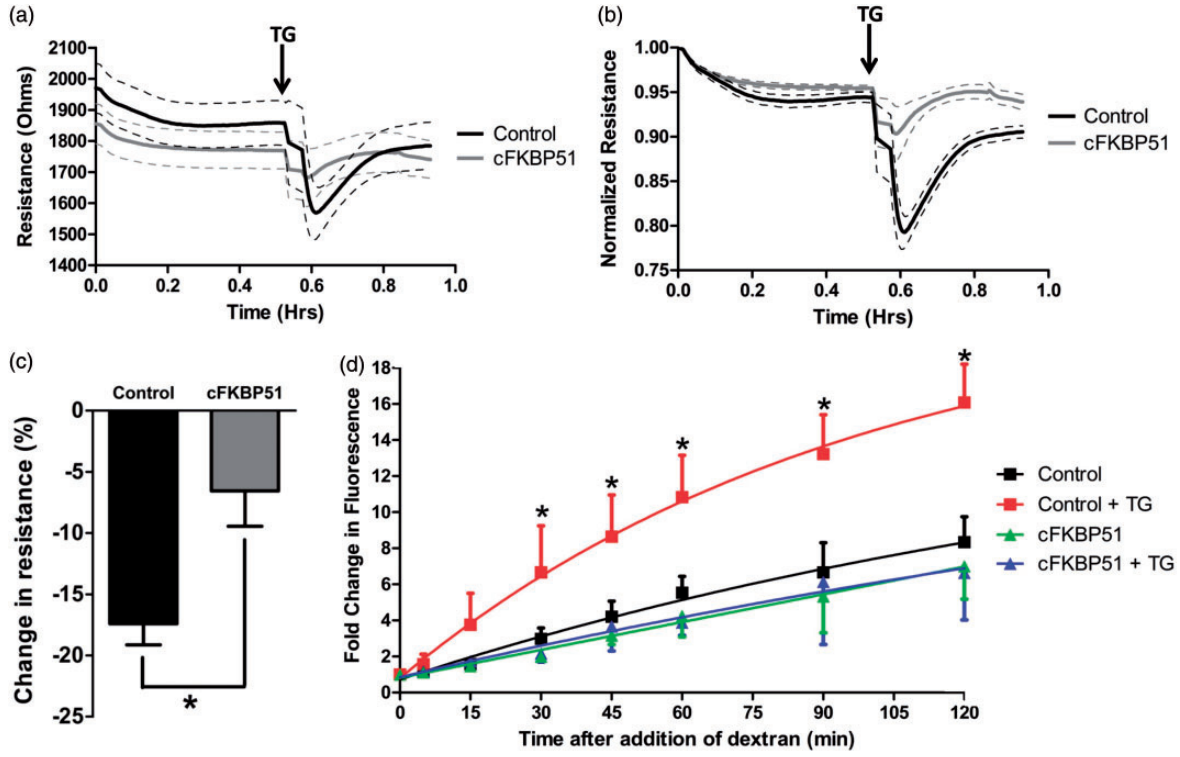

Fig. 7. FKBP51 overexpression protects endothelial barrier integrity and decreases permeability. (a, b) ECIS® was performed to measure changes in endothelial barrier integrity upon activation of calcium entry with thapsigargin. Baseline resistance values were obtained for ~30 min, at which time calcium entry was activated with thapsigargin (1 μM, arrow). (a) Absolute resistance values and (b) normalized, to baseline, resistance values. (c) Bar graph showing maximum change in resistance relative to baseline (0.1 s before addition of thapsigargin) for each cell type. The thapsigargin-induced decrease in resistance was inhibited in cFKBP51 cells. $^*P < 0.05$ as determined by Student's *t*-test; n = 11. (d) Endothelial permeability was measured using the Transwell dextran flux protocol. Calcium entry was activated with thapsigargin (1 μM). While control PAECs exhibited increased permeability following thapsigargin treatment, there was no increase in permeability in cFKBP51 cells. $^*P < 0.05$ for thapsigargin-treated control cells vs. untreated control cells; n = 3–6.

cells, calcium entry through the ISOC channel leads to actin stress fiber formation which contributes to endothelial barrier disruption.

We began our study by characterizing I_{SOC} in terms of its sensitivity to the SOC entry inhibitors 2-APB and YM-58483. 2-APB is considered to be relatively non-specific[26] and can block calcium entry through some TRPC channels.[28–30] On the other hand, YM-58483 is a potent inhibitor of I_{CRAC}.[27] While the endothelial ISOC channel is composed of at least TRPC1 and TRPC4 subunits,[5,31] the CRAC (calcium release activated calcium) channel is composed of orai1 subunits.[44,45] I_{CRAC} is similar to I_{SOC} in that it is a small, non-voltage activated, calcium-selective current.[46] However, the CRAC channel is distinct from the ISOC channel in that it is very highly calcium selective, with an estimated Ca^{2+}:Na^+ permeability ratio of 1000:1 whereas the Ca^{2+}:Na^+ permeability ratio of ISOC is estimated at >10:1.[47] Further, while the CRAC channel is the gold standard of SOC entry channels, it has been questioned as to whether the ISOC channel truly represents a SOC entry channel. For the purpose of our study, it is irrelevant as to whether ISOC is, or is not, store-operated. What is important is that calcium entry through the ISOC channel leads to endothelial barrier disruption[2–4] and that it is inhibited by FKBP51.[10] Here we showed that I_{SOC} is inhibited by 2-APB but not YM-58483, which adds further evidence that the endothelial ISOC channel makeup consists of TRPC1/TRPC4 and not orai1.[2,5,31]

We have previously shown that the large molecular weight immunophilin FKBP51 is a negative regulator of ISOC function.[10] We measure calcium entry through ISOC using patch-clamp electrophysiology. Another method to measure calcium entry is a fluorescence-based approach using a dye such as Fura 2/AM. The difference between the two techniques is that patch-clamp electrophysiology records one current at a time whereas the fluorescence-based approach measures changes in cytosolic calcium that results from activation of a number of different currents. Calcium entry that is measured by the fluorescence-based approach is referred to as global calcium entry. In this study, we observed that FKBP51 inhibits I_{SOC} but does not have a significant effect on the global calcium entry measurement in PAECs. First, this observation suggests that calcium entry through the ISOC

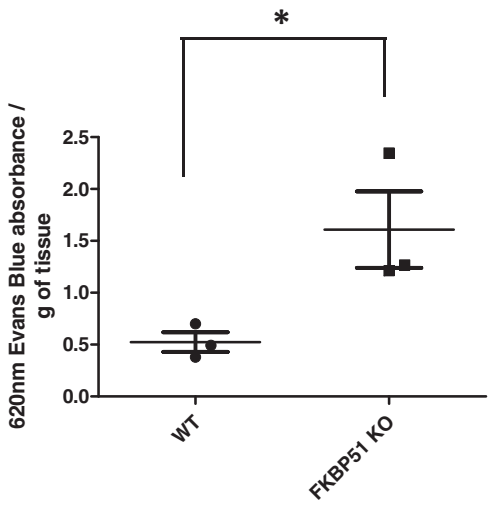

Fig. 8. Knockout of FKBP51 leads to increased calcium entry-induced endothelial permeability *in situ*. An in-chest lung perfusion protocol was performed in which thapsigargin (30 nM) was first perfused to activate calcium entry and was followed by perfusion of Evans Blue dye-conjugated albumin. Endothelial permeability was assessed by measuring tissue permeation of Evans Blue dye-conjugated albumin. Lungs from FKBP51$^{-/-}$ (KO) mice exhibited ~3 times greater permeability following thapsigargin treatment compared to WT mice. Data were analyzed via Student's *t*-test. $^{*}P < 0.05$; n = 3 per group.

channel contributes only a small fraction to the total thapsigargin-induced calcium entry. Second, this observation is consistent with our earlier observations in PAECs which were treated with dexamethasone to upregulate FKBP51 expression.[10] While dexamethasone treatment inhibited I_{SOC}, the global calcium measurement was not significantly decreased compared to control cells. In the same study, overexpression of human FKBP51 in HEK293 cells only modestly decreased the global calcium entry while still inhibiting I_{SOC}. In our experiments, we used thapsigargin to activate I_{SOC}, which activates multiple calcium entry pathways including both store-dependent and store-independent channels.[48] Thus, our observations that FKBP51 inhibits I_{SOC} but not other thapsigargin-activated pathways suggest that FKBP51 is acting specifically on the ISOC channel.

Two major observations in our study were: (1) FKBP51 promotes microtubule polymerization that is critical for the inhibition of I_{SOC}; and (2) FKBP51 inhibits calcium entry-induced actin stress fiber formation. As both microtubule and actin cytoskeletons are influenced by FKBP51, it is worth considering the idea of cross-talk between the actin and microtubule networks in endothelial cells.[49] In human pulmonary artery endothelial cells treated with thrombin, microtubule depolymerization preceded actin stress fiber formation[32,33] and microtubule stabilization decreased actin stress fiber formation.[34] The same effect of microtubule stabilization was also observed in cells treated with TNF-α.[35] An early study by Verin et al.[49] showed that inhibitors of microtubule polymerization increased myosin light chain (MLC) phosphorylation and actin stress fiber formation. They further showed that the increase in MLC phosphorylation was mainly due to decreased myosin-specific phosphatase activity not increased MLC kinase activity, suggesting that microtubules signal to stress fiber formation in a calcium-independent manner. In support of this idea, Birukova et al.[34] subsequently demonstrated a role for Gα12/13 subunits in thrombin-mediated disassembly of microtubules and downstream endothelial barrier disruption. As actin stress fibers can also form in a calcium-dependent manner,[8,38] the question arises as to whether calcium-mediated actin stress fiber formation occurs via cross-talk with microtubules. In the current study, we did not observe a change in microtubules in WT cells following thapsigargin-induced calcium entry (Fig. 4), suggesting that calcium-induced actin stress fibers form independent of microtubule disassembly. However, we cannot discount the possibility that microtubule disassembly did actually occur but had recovered by the time of our measurement, which was at 20 min post thapsigargin treatment. Indeed, Alieva et al.[32] showed microtubule decrease as early as 5 min post thrombin treatment and complete recovery by 60 min. If microtubule disassembly does indeed precede thapsigargin-induced actin stress fiber formation, then the question arises as to whether the FKBP51-mediated increase in microtubule polymerization prevents this disassembly and thereby contributes to the inhibition of actin stress fiber formation. We must therefore consider that the mechanism by which FKBP51 prevents thapsigargin-induced actin stress fiber formation may involve two independent effects by the FKBP51-mediated increase in microtubule polymerization: first, inhibition of calcium influx through the ISOC channel; second, the potential inhibition of microtubule disassembly following calcium entry (Fig. S1). In this study we have demonstrated the role of FKBP51-mediated increase in microtubule polymerization in FKBP51-mediated inhibition of I_{SOC}. Future studies will investigate whether microtubule disassembly is part of calcium-dependent actin stress fiber formation and if so, whether FKBP51-mediated increase in microtubule polymerization can prevent this disassembly leading to decreased actin stress fiber formation.

Another major observation in this study is that FKBP51 plays a protective role against calcium entry-induced endothelial barrier disruption. We observed that overexpression of FKBP51 in PAECs decreased inter-endothelial cell gap formation and permeability compared to WT cells. On the other hand, in FKBP51$^{-/-}$ mice endothelial permeability was increased compared to WT mice, suggesting that the physiological role of FKBP51 is to limit calcium entry-induced endothelial barrier disruption. A potential physiological role of FKBP51 is in acute inflammation where the endothelium transiently and limitedly increases its permeability through a calcium-dependent mechanism[50] to allow leukocytes to reach the site of inflammation.[51] If the limited permeability increase becomes dysregulated, excessive

movement of macromolecules and fluid occurs across the endothelial barrier leading to edema. Indeed, disruption of the FKBP51-mediated inhibition of I_{SOC} may occur in pathophysiological settings such as sepsis or acute illness where patients can experience critical illness related corticosteroid insufficiency (CIRCI).[52–54] As FKBP51 is potently regulated by corticosteroids,[55] it is expected that CIRCI will lead to decreased levels of FKBP51, and decreased FKBP51 expression would allow persistent activation of *I*soc and exacerbated endothelial barrier disruption. While the current study provides biochemical evidence for the FKBP51-mediated inhibition of I_{SOC} and its protection of the endothelial barrier, our future studies will study the role of this pathway in health and disease.

Acknowledgements

The authors would like to thank Linn Ayers and Anna Buford for endothelial cell isolation and culture.

Conflict of interest

The author(s) declare that there is no conflict of interest.

Funding

This work was supported by NIH R01HL107778.

References

1. Ochoa CD and Stevens T. Studies on the cell biology of interendothelial cell gaps. *Am J Physiol Lung Cell Mol Physiol* 2012; 302: L275–286.
2. Cioffi DL, Wu S, Chen H, et al. Orai1 determines calcium selectivity of an endogenous TRPC heterotetramer channel. *Circ Res* 2012; 110: 1435–1444.
3. Wu S, Chen H, Alexeyev MF, et al. Microtubule motors regulate I_{SOC} activation necessary to increase endothelial cell permeability. *J Biol Chem* 2007; 282: 34801–34808.
4. Wu S, Sangerman J, Li M, et al. Essential control of an endothelial cell I_{SOC} by the spectrin membrane skeleton. *J Cell Biol* 2001; 154: 1225–1233.
5. Brough GH, Wu S, Cioffi D, et al. Contribution of endogenously expressed Trp1 to a Ca^{2+}-selective, store-operated Ca^{2+} entry pathway. *FASEB J* 2001; 15: 1727–1738.
6. Cioffi DL, Wu S, Alexeyev M, et al. Activation of the endothelial store-operated ISOC Ca^{2+} channel requires interaction of protein 4.1 with TRPC4. *Circ Res* 2005; 97: 1164–1172.
7. Wu S, Cioffi EA, Alvarez D, et al. Essential role of a Ca^{2+}-selective, store-operated current (I_{SOC}) in endothelial cell permeability: determinants of the vascular leak site. *Circ Res* 2005; 96: 856–863.
8. Moore TM, Brough GH, Babal P, et al. Store-operated calcium entry promotes shape change in pulmonary endothelial cells expressing Trp1. *Am J Physiol Lung Cell Mol Physiol* 1998; 275: L574–582.
9. Zheng J. Molecular mechanism of TRP channels. *Compr Physiol* 2013; 3: 221–242.
10. Kadeba PI, Vasauskas AA, Chen H, et al. Regulation of store-operated calcium entry by FK506-binding immunophilins. *Cell Calcium* 2013; 53: 275–285.
11. Denny WB, Valentine DL, Reynolds PD, et al. Squirrel monkey immunophilin FKBP51 is a potent inhibitor of glucocorticoid receptor binding. *Endocrinology* 2000; 141: 4107–4113.
12. Riggs DL, Roberts PJ, Chirillo SC, et al. The Hsp90-binding peptidylprolyl isomerase FKBP52 potentiates glucocorticoid signaling in vivo. *EMBO J* 2003; 22: 1158–1167.
13. Chambraud B, Belabes H, Fontaine-Lenoir V, et al. The immunophilin FKBP52 specifically binds to tubulin and prevents microtubule formation. *FASEB J* 2007; 21: 2787–2797.
14. Jinwal UK, Koren J 3rd, Borysov SI, et al. The Hsp90 cochaperone, FKBP51, increases Tau stability and polymerizes microtubules. *J Neurosci* 2010; 30: 591–599.
15. Nair SC, Rimerman RA, Toran EJ, et al. Molecular cloning of human FKBP51 and comparisons of immunophilin interactions with Hsp90 and progesterone receptor. *Mol Cell Biol* 1997; 17: 594–603.
16. Reynolds PD, Ruan Y, Smith DF, et al. Glucocorticoid resistance in the squirrel monkey is associated with overexpression of the immunophilin FKBP51. *J Clin Endocrin Metab* 1999; 84: 663–669.
17. Stevens T, Creighton J and Thompson WJ. Control of cAMP in lung endothelial cell phenotypes. Implications for control of barrier function. *Am J Physiol Lung Cell Mol Physiol* 1999; 277: L119–126.
18. Alexeyev MF, Fayzulin R, Shokolenko IN, et al. A retro-lentiviral system for doxycycline-inducible gene expression and gene knockdown in cells with limited proliferative capacity. *Molec Biol Rep* 2010; 37: 1987–1991.
19. Pear WS, Nolan GP, Scott ML, et al. Production of high-titer helper-free retroviruses by transient transfection. *Proc Natl Acad Sci U S A* 1993; 90: 8392–8396.
20. Zufferey R, Nagy D, Mandel RJ, et al. Multiply attenuated lentiviral vector achieves efficient gene delivery in vivo. *Nat Biotechnol* 1997; 15: 871–875.
21. Cioffi DL, Moore TM, Schaack J, et al. Dominant regulation of interendothelial cell gap formation by calcium-inhibited type 6 adenylyl cyclase. *J Cell Biol* 2002; 157: 1267–1278.
22. Cioffi DL, Pandey S, Alvarez DF, et al. Terminal sialic acids are an important determinant of pulmonary endothelial barrier integrity. *Am J Physiol Lung Cell Mol Physiol* 2012; 302: L1067–1077.
23. Villalta PC, Rocic P and Townsley MI. Role of MMP2 and MMP9 in TRPV4-induced lung injury. *Am J Physiol Lung Cell Mol Physiol* 2014; 307: L652–659.
24. Thastrup O, Cullen PJ, Drobak BK, et al. Thapsigargin, a tumor promoter, discharges intracellular Ca^{2+} stores by specific inhibition of the endoplasmic reticulum Ca^{2+}-ATPase. *Proc Natl Acad Sci U S A* 1990; 87: 2466–2470.
25. Xu N, Cioffi DL, Alexeyev M, et al. Sodium entry through endothelial store-operated calcium entry channels: regulation by Orai1. *Am J Physiol Cell Physiol* 2014; 308: C277–288.
26. Putney JW. Pharmacology of store-operated calcium channels. *Mol Interventions* 2010; 10: 209–218.
27. Zitt C, Strauss B, Schwarz EC, et al. Potent inhibition of Ca^{2+} release-activated Ca^{2+} channels and T-lymphocyte activation by the pyrazole derivative BTP2. *J Biol Chem* 2004; 279: 12427–12437.

28. Lievremont JP, Bird GS and Putney JW. Mechanism of inhibition of TRPC cation channels by 2-aminoethoxydiphenylborane. *Mol Pharmacol* 2005; 68: 758–762.
29. Xu SZ, Zeng B, Daskoulidou N, et al. Activation of TRPC cationic channels by mercurial compounds confers the cytotoxicity of mercury exposure. *Toxicol Sci* 2011; 125: 56–68.
30. Xu SZ, Zeng F, Boulay G, et al. Block of TRPC5 channels by 2-aminoethoxydiphenyl borate: a differential, extracellular and voltage-dependent effect. *Br J Pharmacol* 2005; 145: 405–414.
31. Freichel M, Suh SH, Pfeifer A, et al. Lack of an endothelial store-operated Ca^{2+} current impairs agonist-dependent vasorelaxation in $TRP4^{-/-}$ mice. *Nat Cell Biol* 2001; 3: 121–127.
32. Alieva IB, Zemskov EA, Smurova KM, et al. The leading role of microtubules in endothelial barrier dysfunction: disassembly of peripheral microtubules leaves behind the cytoskeletal reorganization. *J Cell Biochem* 2013; 114: 2258–2272.
33. Smurova KM, Biriukova AA, Verin AD, et al. [The microtubule system in endothelial barrier dysfunction: disassembly of peripheral microtubules and microtubules reorganization in internal cytoplasm]. *Tsitologiia* 2008; 50: 49–55.
34. Birukova AA, Birukov KG, Smurova K, et al. Novel role of microtubules in thrombin-induced endothelial barrier dysfunction. *FASEB J* 2004; 18: 1879–1890.
35. Petrache I, Birukova A, Ramirez SI, et al. The role of the microtubules in tumor necrosis factor-alpha-induced endothelial cell permeability. *Am J Resp Cell Mol Biol* 2003; 28: 574–581.
36. Barra HS, Rodriguez JA, Arce CA, et al. A soluble preparation from rat brain that incorporates into its own proteins (14 C)arginine by a ribonuclease-sensitive system and (14 C)tyrosine by a ribonuclease-insensitive system. *J Neurochem* 1973; 20: 97–108.
37. Khawaja S, Gundersen GG and Bulinski JC. Enhanced stability of microtubules enriched in detyrosinated tubulin is not a direct function of detyrosination level. *J Cell Biol* 1988; 106: 141–149.
38. Murphy JT, Duffy SL, Hybki DL, et al. Thrombin-mediated permeability of human microvascular pulmonary endothelial cells is calcium dependent. *J Trauma* 2001; 50: 213–222.
39. Sandoval R, Malik AB, Minshall RD, et al. Ca(2+) signalling and PKCalpha activate increased endothelial permeability by disassembly of VE-cadherin junctions. *J Physiol* 2001; 533: 433–445.
40. Stolwijk JA, Zhang X, Gueguinou M, et al. Calcium signaling is dispensable for receptor regulation of endothelial barrier function. *J Biol Chem* 2016; 291: 22894–22912.
41. O'Mahony L, Akdis M and Akdis CA. Regulation of the immune response and inflammation by histamine and histamine receptors. *J Allergy Clin Immunol* 2011; 128: 1153–1162.
42. Soh UJ, Dores MR, Chen B, et al. Signal transduction by protease-activated receptors. *Br J Pharmacol* 2010; 160: 191–203.
43. Spiegel S and Milstien S. Sphingosine 1-phosphate, a key cell signaling molecule. *J Biol Chem* 2002; 277: 25851–25854.
44. Feske S, Gwack Y, Prakriya M, et al. A mutation in Orai1 causes immune deficiency by abrogating CRAC channel function. *Nature* 2006; 441: 179–185.
45. Vig M, Peinelt C, Beck A, et al. CRACM1 is a plasma membrane protein essential for store-operated Ca^{2+} entry. *Science* 2006; 312: 1220–1223.
46. Rosado JA. Calcium entry pathways in non-excitable cells. *Preface*. Adv Exp Med Biol 2016; 898: vii–viii.
47. Parekh AB and Putney JW Jr. Store-operated calcium channels. *Physiol Rev* 2005; 85: 757–810.
48. Antigny F, Jousset H, Konig S, et al. Thapsigargin activates Ca^{2+} entry both by store-dependent, STIM1/Orai1-mediated, and store-independent, TRPC3/PLC/PKC-mediated pathways in human endothelial cells. *Cell Calcium* 2011; 49: 115–127.
49. Verin AD, Birukova A, Wang P, et al. Microtubule disassembly increases endothelial cell barrier dysfunction: role of MLC phosphorylation. *Am J Physiol Lung Cell Mol Physiol* 2001; 281: L565–574.
50. Huang AJ, Manning JE, Bandak TM, et al. Endothelial cell cytosolic free calcium regulates neutrophil migration across monolayers of endothelial cells. *J Cell Biol* 1993; 120: 1371–1380.
51. Muller WA. Getting leukocytes to the site of inflammation. *Vet Pathol* 2013; 50: 7–22.
52. Annane D, Meduri GU and Marik P. Critical illness-related corticosteroid insufficiency and community-acquired pneumonia: back to the future! *Europ Respir J* 2008; 31: 1150–1152.
53. Cooper MS and Stewart PM. Corticosteroid insufficiency in acutely ill patients. *New Engl J Med* 2003; 348: 727–734.
54. Patel GP and Balk RA. Systemic steroids in severe sepsis and septic shock. *Am J Respir Critical Care Med* 2012; 185: 133–139.
55. Hubler TR and Scammell JG. Intronic hormone response elements mediate regulation of FKBP5 by progestins and glucocorticoids. *Cell Stress Chaperones* 2004; 9: 243–252.